Available online at www.sciencedirect.com
ScienceDirect
ELSEVIER
Sensors and Actuators A 133 (2007) 243–249
SENSORS AND ACTUATORS A PHYSICAL
www.elsevier.com/locate/sna

Implementation of phase-locked loop control for MEMS scanning mirror using DSP

Chuanwei Wang, Hung-Hsiu Yu, Mingching Wu, Weileun Fang *

Department of Power Mechanical Engineering, National Tsing Hua University, Hsinchu, Taiwan

Received 22 November 2005; received in revised form 16 March 2006; accepted 22 March 2006
Available online 2 May 2006

Abstract

The present study has employed the phase-locked loop control method to ensure the operating of MEMS actuators at their resonant frequency. In this study, the control algorism was simulated by the MATLAB. Further, the digital signal processing (DSP) technique was adopted to implement the concept of phase-locked loop control algorithm. Thus, a wide VCO lock-in dynamic range was achieved. In applications, the optical scanners fabricated using the SOI wafer and MOSBE process were respectively employed to demonstrate the present technique. The test show that the resonant frequency was tracked for various driving voltages, loop gains, and initial frequency offsets. Thus, the variation of the scanning angle resulted from the offset of the resonant frequency of the devices can be prevented.
© 2006 Elsevier B.V. All rights reserved.

Keywords: Phase-locked loop; Scanning mirror; Optical MEMS

1. Introduction

The resonance behavior is a useful dynamic characteristic for MEMS devices. This characteristic has been extensively employed to enlarge the output displacement of micro actuators. For instance, the linear displacement of a comb-drive actuator [1] and the scanning angular displacement of a torsional mirror [2] are significantly increased during resonance. This characteristic has been extensively employed in the vibratory MEMS gyroscope [3], the fatigue testing of MEMS devices [4], and the resonant type Coriolis meter as well [5]. However, the resonant frequency of MEMS devices is very sensitive to variations of fabrication, such as the feature size of suspension and the thickness of proof mass. Some technologies are useful to compensate the shift of resonant frequency due to variations of fabrication. Laser trimming removed parts of device so that could compensate shift of resonant frequency [6]. The selective deposited poly-Si on MEMS structures also can compensate the process-induced shift of resonant frequency [7]. The DC bias applied to the actuator could provide the effect of negative spring to compensate the shift of resonant frequency [8]. Moreover, the more critical problems is that the resonant frequency of MEMS devices are also very sensitivity to the environment conditions, such as ambient pressure and temperature. The resonant frequency of MEMS devices will vary with operating time due to the fatigue problem. In addition, the resonant frequency of a non-linear dynamic system may even vary with the operating conditions such as driving voltage [9]. Hence, it is necessary to tune the driving frequency for the aforementioned devices if their resonant frequency is shifted.

Presently, the phase-locked loop (PLL) technology has extensive applications in the area of communication, motor control, etc. In general, a phase-locked loop consists of three main functional components such as voltage-controlled oscillator (VCO), phase detector (PD), and loop filter. A typical second-order spring-mass dynamic system will experience a phase change at its resonant frequency. Thus, the phase change can be detected by the PD, and then controlled. The PLL has frequently been implemented using analog IC, such as NE565 and CD4046. However, an external resistor and capacitor are required to set the frequency of voltage-controlled oscillator (VCO). The PLL can also be implemented by means of software, named software-PLL [10]. To this end, the functions including the mixer, loop filter, A/D converter, and VCO can be properly established and integrated.

* Corresponding author. Tel.: +886 3 5742923; fax: +886 3 5739372.
E-mail address: fang@pme.nthu.edu.tw (W. Fang).

0924-4247/$ – see front matter © 2006 Elsevier B.V. All rights reserved.
doi:10.1016/j.sna.2006.03.026

This study presents a software-PLL control method to ensure the operating of MEMS actuators at their resonant frequency. The digital signal processing (DSP) technique was adopted to implement the concept of phase-locked loop control algorithm. In applications, the scanning mirror operating at resonant frequency is employed to demonstrate the feasibility of the software-PLL control method. Applied proposed method, the resonant frequency of scanner will be tracked to ensure its performance of large scanning angle.

2. Concepts and modeling

The dynamics of a single-degree-of-freedom spring-mass-damping (k-m-c) system can be expressed as the following second-order differential equation,

$$m\ddot{x} + c\dot{x} + kx = F\sin\omega_0 t \tag{1}$$

where F and ω_0 are the amplitude and frequency, respectively, of the external excitation. In this study, the transient response of Eq. (1) is ignored, and the steady-state response of the dynamic system is:

$$x(t) = A\sin\theta(t) = A\sin(\omega_0 t + \phi) \tag{2}$$

where A and ϕ denote the amplitude and phase angle of the response, respectively, and $\theta(t)$ represents the phase of response. The typical variations of amplitude A and phase angle ϕ are shown in Fig. 1 for different ω_0. It is obtained from Fig. 1 that the phase angle will shift for 90° at the resonant point. This characteristic has been employed in this study to trace the resonant frequency of the MEMS device. Hence, the MEMS devices can be operated at their resonant frequency if their phase is locked by control algorithm. This study further implements the concept of software-PLL control algorithm by using a DSP board.

Fig. 2a illustrates the block diagram of a conventional PLL consisting of phase detector, loop filter and VCO. The block diagram in Fig. 2b illustrates the concept to apply the PLL to track the resonant frequency of MEMS resonator [4]. In the present study, the phase angle will vary with time during the tracking of resonant frequency, thus the phase $\theta(t)$ of Eq. (2) can be rewritten as [11],

$$\theta(t) = \omega_0 t + \theta_1(t) \tag{3}$$

where $\theta_1(t)$ is the time varying phase angle. The frequency ω_0 is also regarded as the initial frequency of VCO. In this case, the VCO will provide an output phase $\theta_v(t)$ until the phase angle reach 90°, so as to ensure the MEMS resonator driving at its resonant frequency. The time derivative of $\theta_v(t)$ is expressed as,

$$\frac{d\theta_v(t)}{dt} = \omega_0 + K_2 e(t) \tag{4}$$

where K_2 is the sensitivity (gain) of the VCO. The VCO acts as an integrator, so that the Eq. (4) becomes [11],

$$\theta_v(t) = \omega_0 t + \theta_2(t) \tag{5}$$

where $\theta_2(t)$ is the phase angle of the VCO. To simplify the calculation, an additional gain of $\sqrt{2}$ will add to $y(t)$ before it input to PD. As indicated in Fig. 2b, the output $y(t)$ from PD (which acts as a multiplier) becomes,

$$y(t) = AK_1\{\sin[\theta(t) - \theta_v(t)] + \sin[\theta(t) + \theta_v(t)]\} \tag{6}$$

where K_1 is the VCO output gain. The loop filter, which employed to eliminate the double frequency in Eq. (6), will determine the DC component of the multiplied signals. Thus, the output $e(t)$ from loop filter becomes,

$$e(t) = e(0) + \int_0^t y(t-u) f(u)\,du \tag{7}$$

where $f(t)$ is the impulse function of the loop filter; in addition, the initial condition of loop filter $e(0)$ are zero in this study. After substituting of Eqs. (6) and (7) into Eq. (4) results in,

$$\frac{d\theta_v(t)}{dt} = \omega_0 + K_2 \int_0^t f(t-u) AK_1 \sin[\theta(u) - \theta_v(u)]\,du \tag{8}$$

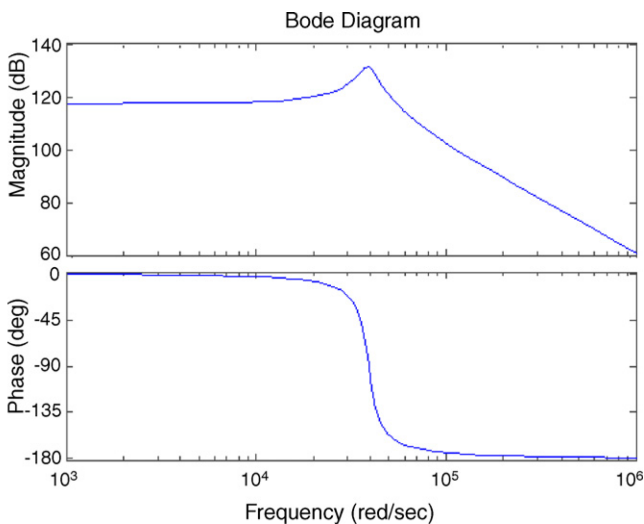

Fig. 1. A typical frequency response and phase change of a dynamic system.

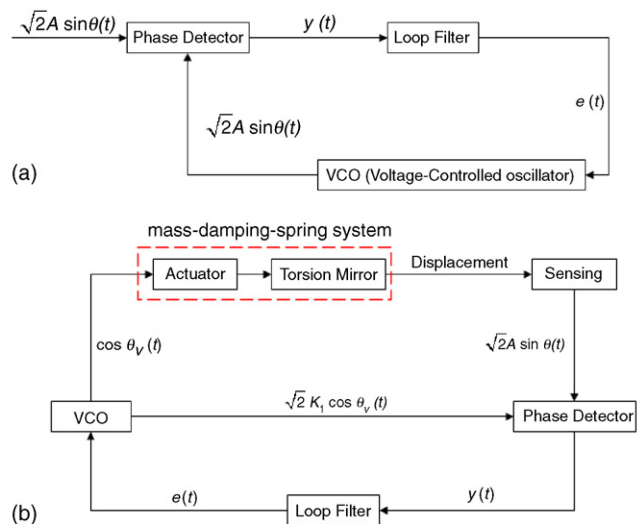

Fig. 2. (a) A typical block diagram of phase-locked loop, and (b) the modification block diagram of phase-locked loop.

Fig. 3. The optical scanners were used to demonstrate the proposed software-PLL technique: (a) the scanner was fabricated on the SOI wafer, and (b) the optical scanner was fabricated using the trench-refilled MOSBE II process.

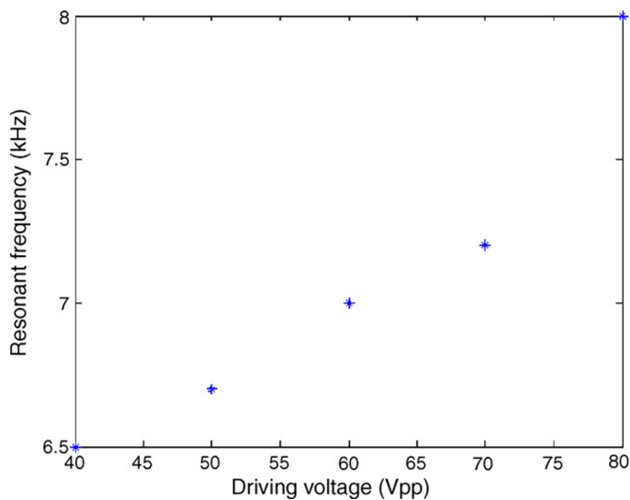

Fig. 4. The measured results of scanning mirror shows the driving voltages will induce the shift of resonant frequency.

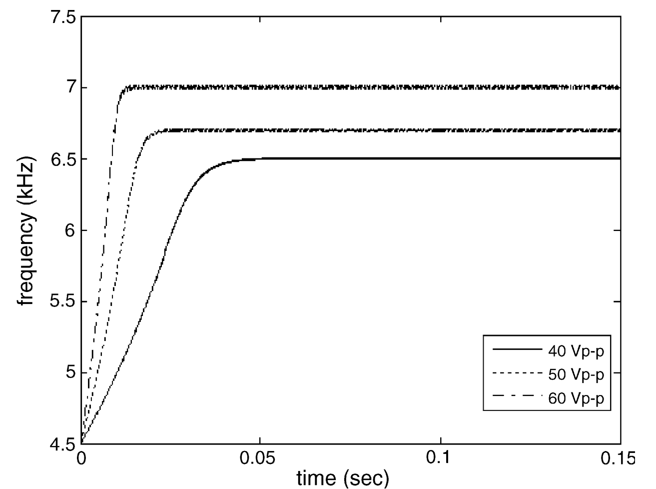

Fig. 5. The simulation results of SOI scanner show the driving frequency was shifted when the driving voltages was changed.

Define the phase error $\psi(t)$ as $\psi(t)=\theta(t)-\theta_v(t)$ is the phase difference between the two signals and the loop gain K as $K=K_1\times K_2$, hence, Eq. (8) can be rewritten as,

$$\frac{d\psi(t)}{dt}=\frac{d\theta(t)}{dt}-\omega_0-AK\int_0^t f(t-u)\sin\psi(u)du \quad (9)$$

Substitution of Eq. (3) into Eq. (9) results in,

$$\frac{d\psi(t)}{dt}=\frac{d\theta_1(t)}{dt}-AK\int_0^t f(t-u)\sin\psi(u)du \quad (10)$$

The impulse function of the loop filter *f*(*t*) in Eq. (7) can be expressed in the following general transfer form,

$$F(s)=\frac{b_0+b_1s+b_2s^2+\cdots+b_ms^m}{a_0+a_1s+a_2s^2+\cdots+a_ns^n} \quad (11)$$

Finally, substitution of Eq. (11) into Eq. (10), the dynamic behavior of the PLL can be expressed as,

$$\left(a_0+a_1\frac{d}{dt}+\cdots+a_n\frac{d^n}{dt^n}\right)\left[\frac{d\psi(t)}{dt}-\frac{d\theta_1(t)}{dt}\right]$$
$$=-AK\left(b_0+b_1\frac{d}{dt}+\cdots+b_m\frac{d^m}{dt^m}\right)\sin\psi(t) \quad (12)$$

According to Eq. (12), the dynamic characteristic of the software-PLL will be influenced by the loop filter. Thus, the pull-in time can be tuned by varying the loop gain *K*. In this study, the PI controller was employed which yielded $F(s)=(s+a)/s$.

3. Applications

In applications, the optical scanners presented in [12,13] were used to demonstrate the proposed software-PLL technique. As shown in Fig. 3, these two optical scanners are consisted of torsional springs, vertical comb actuators, and mirror plate. The scanner in Fig. 3a (SOI scanner) was fabricated on the SOI wafer

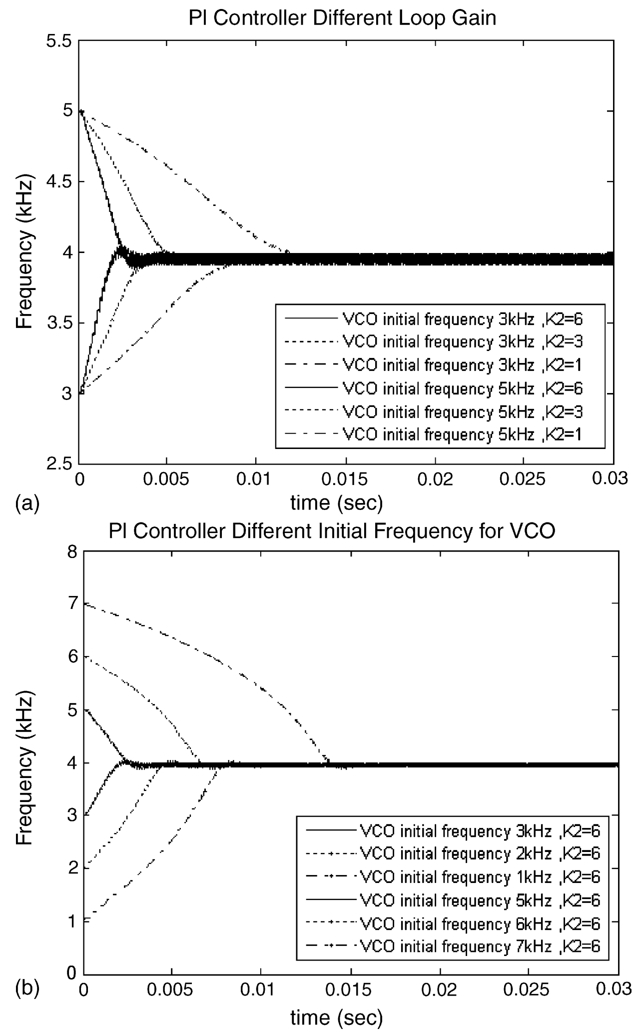

Fig. 6. The simulation results of MOSBE scanner show the driving frequency tracks the resonant frequency of scanner for different gain K_2 and VCO initial frequencies: (a) $K_2=1$, 3, 6, and VCO initial frequencies = 3 kHz, 5 kHz, and (b) $K_2=2$, and VCO initial frequencies ranging from 1 kHz to 7 kHz.

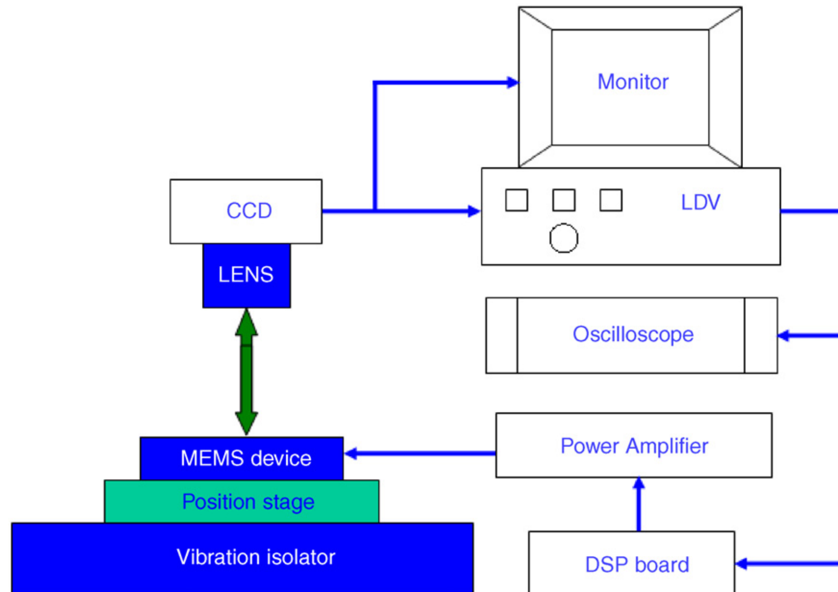

Fig. 7. The testing setup of scanning mirror.

[12], whereas the scanner in Fig. 3b (MOSBE scanner) was fabricated using the trench-refilled MOSBE II process [13]. As indicated by the cross-section illustrations, both of the torsional mirrors were driven with electrostatic force provided by vertical comb actuators. In general, the electrostatic force resulted from the typical electrode design shown in Fig. 3a will introduce an equivalent non-linear spring with negative stiffness [9]. The resonant frequency as well as the maximum scanning angle of this SOI scanner will vary with the driving voltage. The measurement results in Fig. 4 show the resonant frequency of the scanner shifted from 6.5 kHz to 8 kHz when increasing the driving voltage from 40 V to 80 V. As a second example, the MOSBE scanner in Fig. 3b has a special electrode design and will introduce a linear spring [1], so that its resonant frequency (4 kHz) will not vary with the driving voltage. The driving voltage modulation test was applied on the non-linear spring scanner in Fig. 3a. In this case, the software-PLL was employed to enable the scanner operating at its resonant frequency for various driving voltages. The frequency modulation test was applied on the linear spring scanner in Fig. 3b. In this case, the initial frequency of VCO output had a deviation with the resonant frequency of the scanner, so that the software-PLL was used to move the driving frequency towards the central frequency of the VCO. The dynamic range of the PLL was also investigated.

In this study, the zero of PI controller $s = -a$ was selected as $a = 2\pi \times 7000$. In addition, the VCO output gain K_1 was selected as a constant $K_1 = 0.2$, and the sampling time was 50 kHz. The simulation results in Fig. 5 show the driving frequency tracks the resonant frequencies of SOI scanner when driving voltages were 40 V, 50 V, and 60 V, respectively. The resonant frequency of the scanner varied from 6.4 kHz to 7 kHz when the driving voltages increased from 40 V to 60 V. The initial driving frequency for all of these three cases was set at 4.5 kHz, and the resonant frequency of scanner had been tracked within 0.05 s. The simulation results in Fig. 6 show the driving frequency tracks the resonant frequency of MOSBE scanner for different loop gain K_2 and VCO initial frequencies. Fig. 6a shows the driving frequency tracks the resonant frequency of scanner with $K_2 = 1$, 3, and 6, respectively. The results show that it required less than 0.015 s to track the resonant frequency of MOSBE scanner for an initial frequency offset of ±1 kHz (3 kHz and 5 kHz). Fig. 6b shows the driving frequency tracks the resonant frequency of scanner with VCO initial frequencies ranging from 1 kHz to 7 kHz.

The test setup is illustrated in Fig. 7. The vertical comb-drive scanner was initially triggered by an arbitrary waveform generator. The dynamic performances of the scanning mirror were characterized by an optical Laser Doppler Vibrometer (LDV). The results measured by the LDV were then captured and processed by the TI TMS320F2812 DSP processor. This DSP processor consists of a converter (12-bit A/D, D/A) with sampling rate of 50 kHz, a phase detector, a controller, and a VCO. The signal detected from LDV was processed by DSP first, and then output from VCO to drive the vertical comb actuators. The measurement results in Fig. 8 show the driving frequency tracks the resonant frequencies of SOI scanner when driving voltages

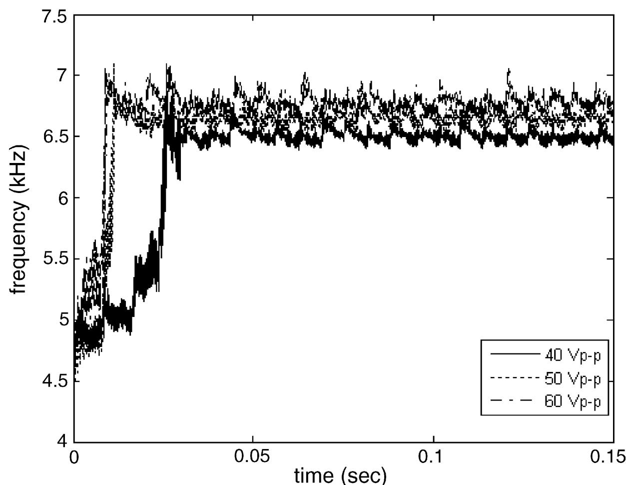

Fig. 8. The measurement results of SOI scanner show the driving frequency was shifted when the driving voltages was changed.

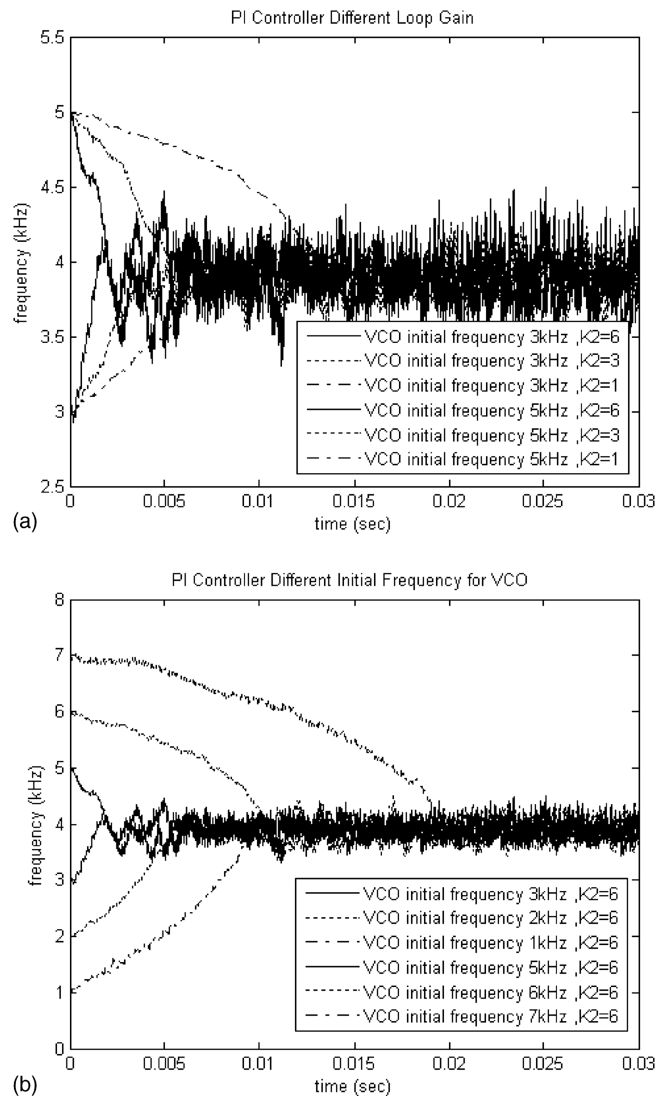

Fig. 9. The measurement results of MOSBE scanner show the driving frequency tracks the resonant frequency of scanner for different gain K_2 and VCO initial frequencies: (a) $K_2 = 1$, 3, 6, and VCO initial frequencies = 3 kHz, 5 kHz, and (b) $K_2 = 2$, and VCO initial frequencies ranging from 1 kHz to 7 kHz.

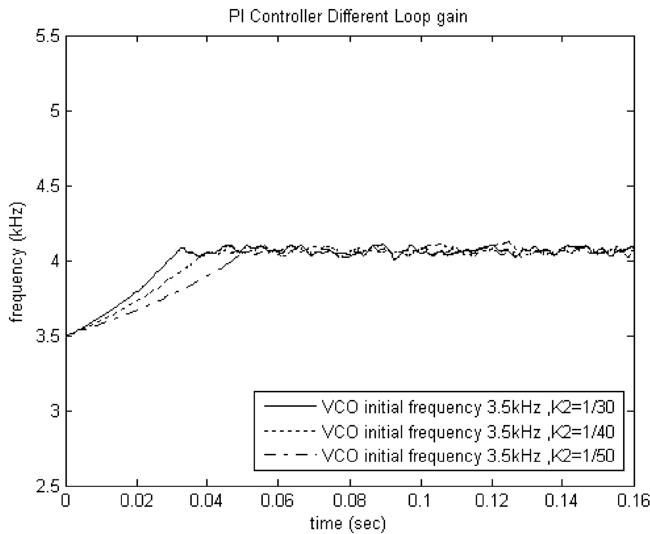

Fig. 10. The measurement results of MOSBE scanner show the driving frequency tracks the resonant frequency of scanner for different gain $K_2 = 1/30$, 1/40 and 1/50 and VCO initial frequency for 3.5 kHz.

were 40 V, 50 V, and 60 V, respectively. The experiment results of Fig. 8 agree well with the simulation ones in Fig. 5. The experiment results in Fig. 9a shows the driving frequency tracks the resonant frequency of MOSBE scanner with $K_2 = 1$, 3, and 6, respectively. The tracking times for these three cases were all less than 0.015 s. Fig. 9b shows the driving frequency tracks the resonant frequency of MOSBE scanner with lock-in range of ±3 kHz. In this experiment, the resonant frequency of the mirror, which was 3.95 kHz, was selected as the central frequency of VCO. The tracking times for these six cases were all less than 0.02 s.

As shown in Fig. 9, at the steady state, the experiment results have a large perturbation of frequency (approximately ±10%) which is resulted from the loop gain difference between experiment and simulation. More specifically, the sensitivity K_2 of VCO is too high ($K_2 = 1$–6) during the experiment to cause the perturbation of steady-state resonance in Fig. 9. As a comparison, the experiment results with lower gain K_2 ($K_2 = 1/50$ to 1/30) are demonstrated in Fig. 10. It is obtained that the perturbation of steady-state resonance is significantly reduced. However, the tracking time required to reach the steady-state frequency will be increased.

4. Conclusions

This study has successfully employed the software-PLL technique to operate the scanning mirror at its resonant frequency. The concept has been implemented using the DSP board. The resonant frequency of the optical scanner influenced by the non-linear spring effect was tracked. In addition, the dynamic characteristics of the scanning mirror influenced by the environment perturbations were also compensated. This technique ensures the MEMS resonator to have a maximum output. The experiment results show that the VCO has a good dynamic range of ±3 kHz. However, the VCO still had significant perturbation of steady-state frequency during tracking. The perturbation of steady-state frequency can be significantly reduced at the cost of longer tracking time. It is possible to employ the fuzzy control algorism to improve the tracking time as well as the steady-state response of the VCO.

Acknowledgements

This paper was (partially) supported by Ministry of Economic Affairs, Taiwan, under contract No. 93-EC-17-A-07-S1-0011, and by National Science Council, Taiwan, under contract NSC 93-2215-E-007-005. The authors would also like to appreciate the NSC Central Regional MEMS Center (Taiwan), the Nano Facility Center of National Tsing Hua University, the LighTuning Technology Inc. for providing the optical scanner, and the NSC National Nano Device Laboratory (NDL) in providing the fabrication facilities.

References

[1] M. Wu, “The Development of Optical MEMS Fabrication—the Case of Micro Scanning Mirror Driven by Electrostatic Comb-driven Actuator.” Ph.D. thesis, Power Mechanical Engineering, National Tsing Hua University, 2005.
[2] H.-Y. Lin, W. Fang, A reinforced micro-torsional-mirror driven by electrostatic torque generators, Sens. Actuators A 105 (2003) 1–9.
[3] R.P. Leland, Adaptive Tuning for Vibration Gyroscopes, in: IEEE Conference on Decision and Control, Orlando, FL, 2001, pp. 3447–3452.
[4] X. Sun, R. Horowitz, K. Komvopoulos, Stability and resolution analysis of a phase-locked loop nature frequency tracking system for MEMS fatigue testing, J. Dynamic Syst., Measure. Ctrl. 124 (2002) 559–605.
[5] J. Kutin, A. Smercnik, I. Bajsic, Phase-locked control of the Coriolis meter’s resonance frequency based on virtual instrumentation, Sens. Actuators A 104 (2003) 86–93.
[6] E.C. Harvey, Laser Micromachining, in: Proceedings of the 1997 IEEE Colloquium on Microengineering Technologies and How to Exploit Them, 1997.
[7] D. Joachim, L. Lin, Characterization of selective polysilicon deposition for MEMS resonator tuning, J. Microelectromech. Syst. 12 (2003) 193–200.
[8] K.B. Lee, Y.-H. Cho, A triangular electrostatic comb array for micromechanical resonant frequency tuning, Sens. Actuators A 70 (1998) 112–117.
[9] V. Kaajakari, T. Mattila, A. Lipsanen, A. Oja, Nonlinear mechanical effects in silicon longitudinal mode beam resonators, Sens. Actuators A 120 (2005) 64–70.
[10] R.E. Best, Phase-Locked Loops: Design, Simulation, and Applications, 5th ed., McGraw-Hill, New York, 2003.
[11] A. Blanchard, Phase-Locked Loops: Applications to Coherent Receiver Design, Wiley and Sons, New York, 1992.
[12] C. Tsou, W.T. Lin, C.C. Fan, B.C.S. Chou, A novel self-aligned vertical electrostatic comb-drives actuator for scanning micromirrors, J. Micromech. Microeng. 12 (2005) 860–885.
[13] M. Wu, C.-F. Lai, W. Fang, Integration of the DRIE, MUMPs, and bulk micromachining for superior micro-optical systems, J. Micromech. Microeng. 15 (2005) 535–542.

Biographies

Weileun Fang was born in Taipei, Taiwan, in 1962. He received his PhD degree from Carnegie Mellon University in 1995. His doctoral research focused on the determining of the mechanical properties of thin films using micromachined structures. In 1995, he worked as a postdoctoral research at Synchrotron Radiation Research Center, Taiwan. He is currently an associate professor at Power Mechanical Engineering Department, National Tsing Hua University, Taiwan. His research interests include MEMS with emphasis on micro optical systems,

microactuators and the characterization of the mechanical properties of thin films.

Chuanwei Wang was born in Taoyuan, Taiwan, in 1978. He received his Master degree from the Mechanical and Mechatronic Engineering Department of National Taiwan Ocean University in 2003. Currently he is studying for the PhD degree in Power Mechanical Engineering Department, National Tsing Hua University, Taiwan. His major research interests include capacitive inertial sensors, capacitive interface circuits, and system control.

Hung-Hsiu Yu was born in Changhua, Taiwan 1976. He received his MS degree from the Mechanical and Mechatronic Engineering Department, National Taiwan Ocean University, Taiwan, in 2002. Currently he is studying for the PhD degree in Power Mechanical Engineering Department, National Tsing Hua University, Taiwan. His research interests include MEMS applications of scanning mirror, dynamic atomic force microscope recording.

Mingching Wu was born in Taoyuan, Taiwan, in 1977. He received the MS and PhD degree in power mechanical engineering (PME), both from the Tsing-Hua University, Hsinchu, Taiwan, in 2001 and 2005, respectively. Currently, he is working as the postdoctoral researcher in PME at Tsing-Hua University. His research interests include novel fabrication process, electrostatic actuator, micro scanning mirror, and optical data storage.